

AperTO - Archivio Istituzionale Open Access dell'Università di Torino

**Direct spectroscopic evidence for binding of anastrozole to the iron heme of human aromatase.  
Peering into the mechanism of aromatase inhibition**

**This is the author's manuscript**

*Original Citation:*

*Availability:*

This version is available <http://hdl.handle.net/2318/91900> since

*Published version:*

DOI:10.1039/c1cc13872c

*Terms of use:*

Open Access

Anyone can freely access the full text of works made available as "Open Access". Works made available under a Creative Commons license can be used according to the terms and conditions of said license. Use of all other works requires consent of the right holder (author or publisher) if not exempted from copyright protection by the applicable law.

(Article begins on next page)



# UNIVERSITÀ DEGLI STUDI DI TORINO

***This is an author version of the contribution published on:***

*Questa è la versione dell'autore dell'opera:*

*[Chem. Commun., 47, 2011, 10.1039/c1cc13872c]*

*ovvero [Sara Maurelli, Mario Chiesa, Elio Giamello, Giovanna Di Nardo, Valentina E. V. Ferrero, Gianfranco Gilardi, Sabine Van Doorslaer, 47, RSC, 2011, 10737 – 10739]*

***The definitive version is available at:***

*La versione definitiva è disponibile alla URL:*

*[<http://pubs.rsc.org/en/journals/journalissues/cc#!recentarticles&all>]*

# Direct Spectroscopic Evidence for Binding of Anastrozole to the Iron Heme of Human Aromatase. Peering into the Mechanism of Aromatase Inhibition

Sara Maurelli<sup>a</sup>, Mario Chiesa<sup>a\*</sup>, Elio Giamello<sup>a</sup>, Giovanna Di Nardo<sup>b</sup>, Valentina E. V. Ferrero<sup>b</sup>, Gianfranco Gilardi<sup>b</sup>, Sabine Van Doorslaer<sup>c</sup>

**Aromatase (CYP19A1), is a microsomal cytochrome P450 catalysing the conversion of androgens to estrogens. Non-steroidal inhibitors, such as anastrozole, are important drugs in breast cancer therapy. Using hyperfine sublevel correlation (HYSCORE) spectroscopy we provide the first experimental evidence of the binding of anastrozole to the iron heme of human aromatase.**

One of the major goals for cancer treatment is the identification of enzyme targets and the development of specific and effective inhibitor-based drugs. For this purpose, the knowledge of how the inhibitor interacts with the protein and modifies its catalytic properties is crucial for the rational design of new and effective inhibitors. Detailed information on the structure-function relationship is, however, often difficult to obtain, in particular in the absence of the crystal structure of the enzyme-inhibitor complex.

One such case is that of aromatase (CYP19A1), a microsomal cytochrome P450 catalysing the conversion of androgens (androstenedione, testosterone, and 16 $\alpha$ -hydroxytestosterone) to estrogens (estrone, 17 $\beta$ -estradiol, and 17 $\beta$ , 16 $\alpha$ -estriol, respectively).<sup>1</sup>

In the human body, aromatase is pathologically over-expressed in estrogen-dependent tumors, including breast cancer. For this reason it represents an optimal target for breast cancer therapy. To date, three aromatase inhibitors (AIs) have been approved by the U.S. Food and Drug Administration and they are currently used for the treatment of breast cancer in post-menopausal women. They are classified as third generation AIs and include the steroidal molecule exemestane (Aromasin) and two non-steroidal molecules, anastrozole (Arimidex) and letrozole (Femara). Exemestane is a mechanism-based irreversible inhibitor.<sup>2,3</sup>

Anastrozole (see inset in Figure 1) and letrozole, contain a triazole functional group and they act as competitive inhibitors perturbing the catalytic properties of the heme prosthetic group.<sup>4</sup>

Docking studies have proposed a possible binding mode of anastrozole and letrozole in the active site of aromatase.<sup>5,6</sup> However, no direct experimental evidence is currently available for the interaction between the heme catalytic center of human aromatase and non-steroidal inhibitors. Electron Paramagnetic Resonance (EPR) spectroscopy has since many years been one of the most useful tools for characterizing ferric hemoproteins<sup>7,8</sup>. Here, we report, as part of a systematic study of aromatase, a combined Continuous Wave (CW)-EPR and Hyperfine Sublevel Correlation spectroscopic (HYSCORE) analysis of the ferric form of aromatase in frozen solution and the first experimental evidence of the binding of anastrozole to the heme active centre of human aromatase.

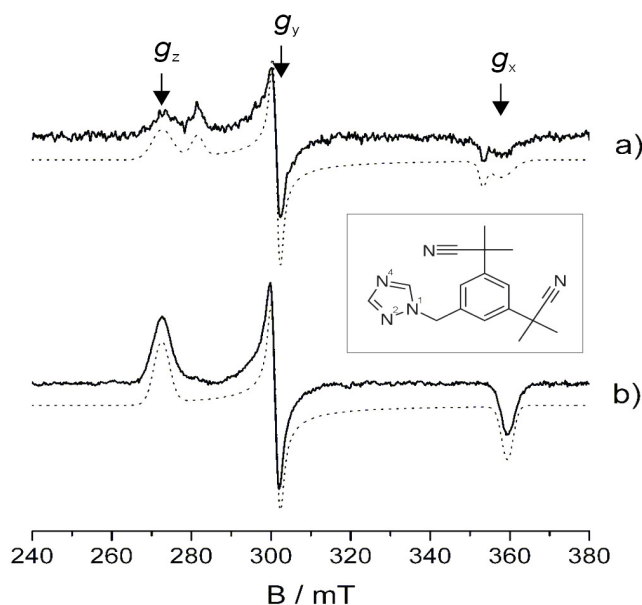


**Figure 1.** Experimental (full line) and simulated (dotted line) X-band CW-EPR of a frozen solution of a) aromatase and b) aromatase co-purified with anastrozole. The protein buffer is 100 mM potassium phosphate pH 7.4, 20% glycerol, 0.1% Tween 20, 1  $\mu$ M  $\beta$ -mercaptoethanol. T = 77K. In the inset the chemical formula of 2-[3-(1-cyano-1-methyl-ethyl)-5-(1H-1,2,4-triazol-1-ylmethyl)phenyl]-2-methyl-propanenitrile (anastrozole, Arimidex) is shown.

The enzyme was cloned and expressed in a soluble form in *E. coli*. The protein was purified in absence and in presence of

saturating amounts of the inhibitor anastrozole (1  $\mu\text{M}$ ). The protein was then concentrated for spectroscopic means. The UV-vis spectrum of aromatase shows a Soret peak at 418 nm, that shifts to 422 nm when anastrozole is present (Supporting Information). This red shift, also known as “type II” spectral shift, is associated to the binding of a N containing ligand to the heme iron of cytochrome P450s<sup>9</sup>.

Figure 1 shows the experimental X-band (9.5 GHz) CW-EPR spectra of frozen solutions of 580  $\mu\text{M}$  substrate-free ferric aromatase (Figure 1a) and of 490  $\mu\text{M}$  ferric aromatase/anastrozole (Fig. 1b). The characteristic EPR features of low-spin ( $S=1/2$ ) Fe(III) heme centers dominate the spectra in both the absence and presence of anastrozole. The EPR spectrum of the substrate-free protein indicates the presence of two different species, characterized by slightly different  $g$  factors (Table 1). This observation agrees with previous reports<sup>10,11</sup> and in this respect, aromatase resembles highly purified P450scc and a mutant of P450cam,<sup>12</sup> where multiple low-spin species have been observed.

Upon binding of anastrozole (Figure 1b) only a single contribution is observed in the CW-EPR spectrum. These changes in CW-EPR spectrum together with the red shift of the Soret peak (Supporting Information) indicate a modification in the local coordination environment of the heme center upon anastrozole addition. To better understand the local coordination environment of the heme iron prior to and after interaction with anastrozole, X-band HYSCORE spectra were recorded at different field positions (Figure 2 and Supporting Information).

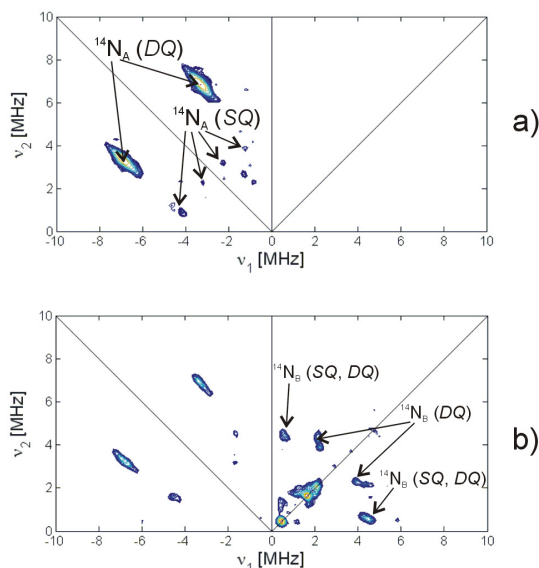


**Figure 2.**  $^{14}\text{N}$  HYSCORE spectra recorded at the field position corresponding to the  $g_y$  feature ( $B_0 = 309.5$  mT) and  $\tau = 176$  ns for frozen solutions of a frozen solution of a) substrate-free ferric aromatase, and b) ferric aromatase in the presence of anastrozole. The spectra are recorded at  $T = 7\text{K}$ .  $N_A$  and  $N_B$  indicate the porphyrin and anastrozole nitrogens respectively.

	$g_x$ $\pm 0.002$	$g_y$ $\pm 0.002$	$g_z$ $\pm 0.001$		$ A_x $ $\pm 0.1$	$ A_y $ $\pm 0.1$	$ A_z $ $\pm 0.1$	$\alpha\beta\gamma$	$ e^2qQh $	$\eta$	$\alpha'\beta'\gamma'$
Aromatase	1.899	2.255	2.493	$N_A$	4.8	4.3	6.0	$0,15\pm 5,0$	$1.8\pm 0.1$	$0.10\pm 0.05$	$0, 75\pm 10, 0$
Aromatase +	1.924	2.254	2.415	$N_A$	4.8	4.3	6.0	$0,15\pm 5,0$	$1.8\pm 0.1$	$0.10\pm 0.05$	$0, 75\pm 10, 0$
anastrozole	1.890	2.255	2.493	$N_B$	2.0	2.0	0.8	$0,0,0$	$2.8\pm 0.3$	$0.35\pm 0.02$	$30\pm 5,5\pm 3,45\pm 5$

**Table 1.** Spin Hamiltonian parameters derived from the spectra reported in Figures 1 and 2.  $^{14}\text{N}$  hyperfine and nuclear quadrupole couplings are given in units of MHz. Euler angles are in degrees.

The (-,+) quadrant of the HYSCORE spectrum of substrate-free aromatase taken at an observer position corresponding to  $g=g_y$  (Figure 2a) is dominated by cross peaks at about (-6.8, 3.2), (-3.2, 6.8) MHz, due to strongly coupled nitrogen nuclei (labelled as  $N_A$ ). These frequencies are the double-quantum (DQ) transitions of the four approximately equivalent nitrogen nuclei of the porphyrin ring.<sup>13,14</sup> Computer simulation of the spectra at different observer positions (see Supporting Information) allows extracting the full hyperfine and nuclear quadrupole tensors reported in Table 1. The values agree with those found for the pyrrole nitrogens of other ferric heme proteins.<sup>14-16</sup>

Upon addition of anastrozole to the protein, the HYSCORE spectrum recorded at the same field position (Figure 2b) shows new cross peaks in the (+,+) quadrant that originate from the interaction of the unpaired electron with a new  $^{14}\text{N}$  nucleus. The two cross peaks in the (+,+) quadrant centered at about (2.3, 4) MHz and (4, 2.3) MHz (labelled as  $N_B$ ) are assigned to double-quantum transitions of a weakly coupled nitrogen, while cross peaks at  $\sim(-0.6, 4.4)$  MHz and  $\sim(4.4, 0.6)$  MHz correspond to

combinations of single-quantum – double-quantum ( $SQ$ ,  $DQ$ ) transitions. The remarkable spectral resolution of the HYSORE spectra of the aromatase-anastrozole complex (Figure 2b and Supporting Information) leads to the determination of the full hyperfine coupling and nuclear quadrupole coupling (nqc) tensor of this new  $^{14}\text{N}$  (Table 1). The hyperfine values are smaller (in absolute value) than those found for the iron-binding imidazole nitrogens of bis-histidine-coordinated heme centers  $^{14,15}$ , but agree remarkably well with those reported for N(His) of the myoglobin-mercaptoethanol complex ( $|A|=[2.6,2.6,1.4]$  MHz,  $|e^2qQ/h|=2.5$  MHz,  $\eta=0.3$ ).<sup>17</sup> The principal  $g$  values of the latter complex (2.41, 2.24, 1.93)<sup>17</sup> are also similar to the ones found for the aromatase - anastrozole complex (Table 1). Furthermore, hyperfine values of  $\sim 2$  MHz have been reported for the axial amine's nitrogen in imidazole-heme-mercaptoethanol and in pyridine-heme-mercaptoethanol complexes.<sup>18</sup> This not only gives strong evidence that anastrozole is binding to the heme iron of the aromatase, it also suggests that the coordination is occurring *via* N-4 of the triazole ring. The possibility of coordination to the heme iron by a histidine residue was ruled out due to both the high distance of all histidine residues from the heme (ranging from 13 to 31 Å) and the retained ability of the reduced iron to bind CO giving a Soret band at 450 nm, typical of the thiolate-ligated heme proteins (see Supporting Information). Reported nuclear coupling values for 1H-1,2,4 triazole<sup>19</sup> are ( $|e^2qQ/h|=4.2$  MHz  $\eta=0.7$ ) and ( $|e^2qQ/h|=3.2$  MHz  $\eta=0.1$ ) for N<sup>2</sup> and N<sup>4</sup>, respectively. The latter value is similar to the one observed for the imidazole.<sup>20</sup> Addition of a Lewis acid (heme) to an amine leads to a reduction of the electric field gradient at the nitrogen nucleus,<sup>21</sup> explaining the  $|e^2qQ/h|$  value extracted from the HYSORE spectra (2.5 MHz). This value is consistent with nqc tensors measured for the N(His) of the myoglobin-mercaptoethanol complex<sup>17</sup> and metal-coordinated nitrogens in different ligands, including imidazole, studied by nuclear quadrupole resonance.<sup>21,22</sup> The important feature to be emphasized from these studies is that  $e^2qQ/h$  values of the order of those measured in our case are associated to the “lone pair” nitrogen donor orbital defining the the principal axis of the nqc tensor ( $Q_{zz}$ ). This orbital is axially directed towards the empty iron  $d_z^2$  orbital forming a  $\sigma$  bond lying along the normal to the heme plane. Simulation of the HYSORE spectra (Supporting Information) demonstrates that  $Q_{zz}$  is nearly aligned along  $g_{zz}$  ( $0 < \beta < 10^\circ$ ), indicating that the axial nitrogen ligand is directed close to the heme normal, forming an end-on complex.

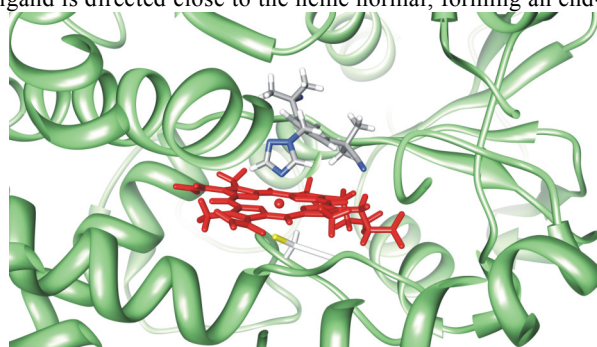


**Figure 3.** Docking model of human aromatase-anastrozole complex generated by Swiss Dock server (<http://www.swissdock.ch/>). Anastrozole is shown in grey with nitrogen atoms in blue. Heme is shown in red and the fifth iron ligand, the sulfur atom of cysteine 437, is shown in yellow.

A schematic docking model representative of the above discussed HYSORE results and illustrating the binding of anastrozole to the active site of human aromatase is shown in Figure 3 and corresponds to earlier reported binding themes of triazoles to other heme proteins.<sup>23,24</sup> It should be noted that, even though the binding of anastrozole to the heme iron via N<sup>4</sup> has been suggested by previous docking studies,<sup>5</sup> the model shown in Figure 3, based on the crystal structure of human aromatase<sup>3</sup> (3EQM), is for the first time, directly supported by experimental evidence.

In summary, we have determined by means of  $^{14}\text{N}$  HYSORE spectroscopy the features of a weakly coupled nitrogen upon interaction of human aromatase with anastrozole. Detailed analysis of the HYSORE spectra strongly supports formation of a complex between the ferric heme centre of aromatase and anastrozole, providing information on the molecular mechanism by which inhibition of the protein functions is induced by the inhibitor. This observation is of interest in the context of the design and development of other, specific inhibitors.

## Notes and references

<sup>a</sup> Dipartimento di Chimica IFM, Università di Torino and NIS, Nanostructured Interfaces and Surfaces Centre of Excellence, Via P. Giuria 7, I - 10125 Torino, Italy E-mail: [m.chiesa@unito.it](mailto:m.chiesa@unito.it)

<sup>b</sup> Dipartimento di Biologia Animale e dell'Uomo, Università di Torino, Via Accademia Albertina 13, Torino, Italy

<sup>c</sup> University of Antwerp, Department of Physics, Universiteitsplein 1, B-2610 Wilrijk-Antwerp, Belgium

† Electronic Supplementary Information (ESI) available: Uv-Vis spectra of aromatase and aromatase-anastrozole complex. Details of experimental methods. Experimental and computer simulated HYSORE spectra at different observer positions. Difference UV-Vis spectra of reduced CO complex. See DOI: 10.1039/b000000x/

‡ We thank Ms Alice Bracco for helping in the preparation of the samples.

- 1 E. R. Simpson, M. S. Mahendroo, G. D. Means, M. W. Kilgore, M. M. Hinshelwood, S. Graham-Lorence, B. Amarnah, Y. Ito, C. R. Fisher, M. D. Michael, C. R. Mendelson, S. E. Bulun, *Endocr. Rev.*, 1994, **15**, 342.
- 2 Y. Hong, B. Yu, M. Sherman, Y. C. Yuan, D. Zhou, S. Chen, *Mol. Endocrinol.*, 2007, **21**, 401.
- 3 D. Ghosh, J. Griswold, M. Erman, W. Pangborn, *Nature*, 2009, **457**, 219.

- 
- 4 Y. C. Kao, L. L. Cam, C. A. Laughton, D. Zhou, S. Chen, *Cancer Res.*, 1996, **56**, 3451.
  - 5 Y. Hong, L. Hongzhi, Y. C. Yuan, S. Chen, *Steroid Enzymes and Cancer. Ann. NY Acad. Sci.*, 2009, **1155**, 112.
  - 6 Y. Hong, R. Rashid, S. Chen, *Steroids* 2001, **76**, 802.
  - 7 A. F. Walker, *Coord. Chem. Rev.*, 1999, **185-186**, 471.
  - 8 G. Zoppellaro, K. L. Bren, A. A. Ensign, E. Harbitz, R. Kaur, H. P. Hersleth, U. Ryde, L. Hederstedt, K. K. Andersson, *Biopolymers*, 2009, **91**, 1064.
  - 9 C. R. Jefcoate, *Methods Enzymol.*, 1978, **52**, 258.
  - 10 S. L. Gantt, I. G. Denisov, Y. V. Grinkova, S. G. Sligar, *Biochem. Biophys. Res. Commun.*, 2009, **387**, 169.
  - 11 N. Kagawa, H. Hori, M. R. Waterman, S. Yoshioka, *Steroids*, 2004, **69**, 235.
  - 12 K. Takeuchi, M. Tsubaki, J. Futagawa, F. Masuya, H. Hori, *J. Biochem.*, 2001, **130**, 789.
  - 13 E. Vinck, S. Van Doorslaer, *Phys. Chem. Chem. Phys.*, 2004, **6**, 5324.
  - 14 I. García-Rubio, J. I. Martínez, R. Picorel, I. Yruela, P. J. Alonso, *J. Am. Chem. Soc.*, 2003, **125**, 15846.
  - 15 E. Vinck, S. Van Doorslaer, S. Dewilde, G. Mitrikas, A. Schweiger, L. Moens, *J. Biol. Inorg. Chem.*, 2006, **11**, 467.
  - 16 T. C. Yang, R. L. McNaughton, M. D. Clay, F. E. Jenney, R. Krishnan, D. M. Kurtz, M. W. W. Adams, M. K. Johnson, B. M. Hoffman, *J. Am. Chem. Soc.*, 2006, **128**, 16566.
  - 17 R. S. Magliozzo, J. Peisach, *Biochemistry*, 1993, **32**, 8446.
  - 18 J. Peisach, W. B. Mims, J. L. Davis, *J. Biol. Chem.*, 1979, **254**, 12379.
  - 19 H. M. Palmer, D. Stephenson, J. A. S. Smith, *Chem. Phys.*, 1985, **97**, 103.
  - 20 M. L. S. Garcia, J. A. S. Smith, P. M. G. Bavin, C. R. Ganellin, *J. Chem. Soc. Perkin Trans. II*, 1983, 1391.
  - 21 Y. N. Hsieh, G. V. Rubenacker, C. P. Cheng, T. L. Brown, *J. Am. Chem. Soc.*, 1977, **99**, 1384.
  - 22 C. I. H. Ashby, C. P. Cheng, T. B. Brown, *J. Am. Chem. Soc.*, 1978, **100**, 6057; G. V. Rubenacker, T. L. Brown, *Inorg. Chem.*, 1980, **19**, 392.
  - 23 G. Roman, M. N. Rahman, D. Vukomanovic, Z. Jia, K. Nakatsu, W. A. Szare, *Chem. Biol. Drug. Des.*, 2010, **75**, 68.
  - 24 L. M. Podust, T. L. Poulos, M. R. Waterman, *Proc. Natl. Acad. Sci.*, 2001, **98**, 3068.